Estimation of Rainfall on the Japanese Islands and Their Adjacent Ocean from Satellite (GMS) Infrared Imagery

AUTHOR(S):

XIE, Pingping

CITATION:

XIE, Pingping. Estimation of Rainfall on the Japanese Islands and Their Adjacent Ocean from Satellite (GMS) Infrared Imagery. Bulletin of the Disaster Prevention Research Institute 1992, 42(1): 1-18

ISSUE DATE:

1992-03

URL:

http://hdl.handle.net/2433/124984

Bull. Disas. Prev. Res. Inst., Kyoto Univ., Vol. 42, Part 1, No. 363, March, 1992

Estimation of Rainfall on the Japanese Islands and Their Adjacent Ocean from Satellite (GMS) Infrared Imagery

By Pingping XIE

(Manuscript received on Jan. 14, 1992; revised on Feb. 17, 1992)

Abstract

The method developed for estimating rainfall over several sample areas over the main islands of Japan from IR imagery data of GMS is extended to estimate rainfall over a wider region including the Japanese islands and their adjacent ocean. In this method, rainfall estimation over a grid of 1.25° latitudes × 1.25° longitudes is made by assuming linear relations between hourly rainfall and cold cloud fractional coverage (FC) for the 3 rain cloud types (A: Cumulus; B: Cumulonimbus and C: Middle Clouds) and assuming rain free in cases of cloud amount less than 70% as well as cloud type D (Cirrus). The threshold temperatures to define FC for the 3 rain cloud types are kept the same as those used in Xie[7], that is, 245 K, 235 K and 255 K for each cloud type A, B and C, respectively. The proportional constants between hourly rainfall and FC are assumed to be functions of latitude and are calculated by using the rainfall data obtained by radar-AMeDAS composite and FC data of the grids over the Japanese islands. The resultant relative errors of rainfall estimation over the Japanese islands are 73% and 17% for daily and monthly estimation, respectively, which satisfy the useful level of the accuracy of rainfall data in climatic use.

1. Introduction

The requirements to derive global rainfall distribution come from many fields of meteorology and climatology. The rainfall over land can be observed directly from networks comprising raingages and weather radars. However rainfall data over the ocean are hard to obtain without the aid of satellite observation.

Among infrared (IR), visible (VIS) and passive microwave (PM) data available from the present satellite observation which can be used to detect rainfall, IR data are the most hopeful in estimating rainfall on a climatic scale, eventhough it is applied only by an indirect method (Barrett and Martin[1], Arkin and Ardanuy[2]). The IR techniques, such as those developed by Griffith et al.[3] and Arkin and Meisner[4], provide good estimations of rainfall in the tropical areas where convective clouds dominate. However, it is much more difficult to estimate rainfall in mid-latitudes from IR data, because non-raining cirrus and raining stratiform clouds with lower cloud tops are often observed (Xie and Mitsuta[5]). Therefore, it is necessary to introduce the cloud type information in the rainfall estimation in mid-latitudes from satellite-observed IR data.

The present author (Xie[6], Xie[7]) has developed a method to estimate rainfall in five areas of about 10^4 km^2 over the main islands of Japan from GMS (Geostationary Meteorological Satellite) IR data, using T_{BB} histogram and cloud type information de-

rived by a discriminate analysis technique. A further step toward practical application of this IR rainfall estimation method is to adjust the method to cover a wider area, because the method was developed originally for areas with similar weather conditions on the main islands of Japan.

The present paper intends to extend the method for the estimation of rainfall in June 1989 over a region of 23.75° latitudes × 27.5° longitudes surrounding Japan with spatial resolution of 1.25° latitudes × 1.25° longitudes.

2. Method of Rainfall Estimation

Xie[6] developed a method to estimate total cloud amount and to discriminate cloud type for areas of about 10^4 km^2 with similar weather conditions on the Japanese main islands using only GMS IR data. Following that study, Xie[7] developed a method to estimate the area-averaged rainfall for the same areas from the T_{BB} histograms and the cloud type derived from the IR data. The fundamental procedures to estimate rainfall from IR imagery data in this method are as follows;

1) Estimate total cloud amount of the target area from T_{BB} histogram by the method developed in Xie[6], which takes account of the ground-related spectral peak and the partially cloud-covered pixels. Define the case with cloud amounts smaller than 0.3 as Clear Sky (Type S), case between 0.3 and 0.7 as Fine (Type F) and case equal to or larger than or 0.7 as cloudy case.
2) In the cloudy case with cloud amounts equal to or larger than 0.7, classify clouds into four types A: cumulus, B: cumulonimbus, C: middle clouds and D: high clouds from the selected 4 IR cloud feature parameters (see **Table 3** in Xie[6]) by using discriminate analysis technique.
3) Estimate hourly rainfall for each area by using the cloud type information and T_{BB} histogram. The cases with cloud type of S (Clear Sky), F (Fine) or D (High Clouds) are assumed to be rain free and the hourly rainfall for the rain cases (Type A, B and C) are calculated from fractional coverage (FC) of clouds with cloud top colder than a certain threshold temperature in the area by applying linear relations shown in **Table 1**. The threshold temperatures and proportional contants shown in **Table 1** were determined by calculating the linear regression between area-averaged rainfall and cold cloud fractional coverage from GMS IR data. Estimation of rainfall for a longer period is made by accumulating the hourly estimations for the period.

Table 1. Thresholds and Regressional Equations Used in Xie[7]

TYPE	THRESHOLD	REGRESSIONAL EQUATIONS
A	245 K	$E_I = 2.527 \cdot FC_A$
B	235 K	$E_I = 2.820 \cdot FC_B$
C	255 K	$E_I = 1.238 \cdot FC_C$

E_I : IR estimation of hourly rainfall in mm
FC: cloud fractional coverage colder than the threshold

3. Data

The GMS IR imagery data and radar-AMeDAS composite rainfall data of the First Algorithm Intercomparison Program (AIP-1) data set of GPCP (Global Precipitation Climate Project) are used in the present study. The data area extends from 120°E-147.5°E, 22.5°N-46.25°N, as shown in **Fig. 1**, and the data period covers one month from 1 to 30 June, 1989. The precipitation in this period over the area is mainly from the Baiu front and a tropical depression.

As the method described in Xie[6] and Xie[7] was originally developed for areas of about 10^4 km^2 over the main islands of Japan, the entire area of AIP/1 as shown in **Fig. 1** is divided into 22×19 meshes of 1.25° latitudes × 1.25° longitudes in area and rainfall is estimated for each mesh.

The data set includes 720 hourly GMS IR observations in the 30 day period, from 00Z 1 to 23Z 30 June, 1989. The original GMS VISSR IR data have been interploted into a form so that each pixel has a spatial resolution of 0.05° latitude × 0.065° longitude, the total IR pixel number in each mesh being 500. IR data at each pixel is in digital form ranging from 0 to 255, which can be converted into equivalent blackbody temperature, T_{BB}, by referring to the calibration table in the data file. In order to estimate the total cloud amount and to discriminate cloud type, T_{BB} histograms are constructed and the 4 IR cloud feature parameters (see **Table 3** in Xie[6]) are calculated for every mesh.

The data set of Radar-AMeDAS rainfall is used as the ground truth of rainfall in the present study, which includes 720 hourly rainfall distributions obtained by raingages

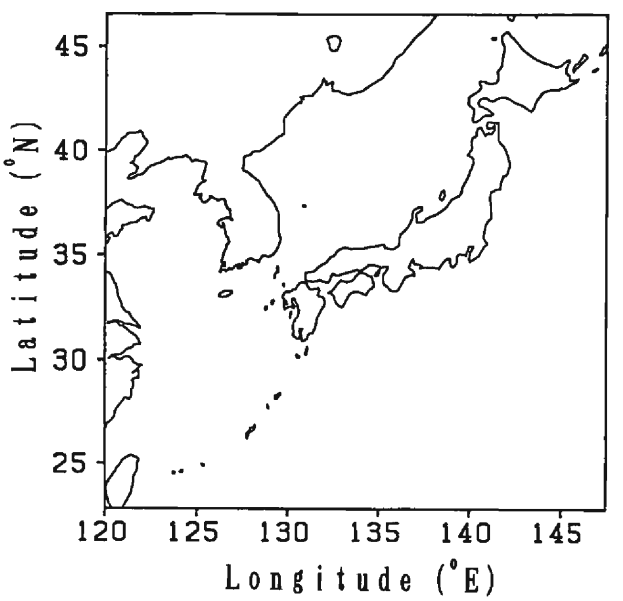

Fig. 1. The investigation area of GPCP-AIP/1.

of the AMeDAS network supplemented by weather radar observation (Takemura[8]) for the period. The network constituting 22 weather radar stations and about 1300 AMeDAS raingages supplies a reliable ground truth of the rainfall over and near the main islands of Japan. The rainfall data used here have the same spatial resolution as that of the IR data. In the present study, the areal-averaged rainfall in each mesh of 1.25° latitudes × 1.25° longitudes is calculated and employed as the ground truth.

4. Extension of the Estimation Method

Among the all of the procedures of rainfall estimation described in section 2, discrimination of cloud type and derivation of rainfall may be the most sensitive to geographic changes. For this reason, the method of discrimination of cloud type is first tested with the present data set. The results showed a high ratio of agreement of about 70% when compared with the concurrent subjective cloud type composed by the Meteorological Satellite Center of Japan meteorological agency (JMA) for several meshes in the area. This ratio of agreement may be high enough to reliably apply the original method to the whole area.

The necessary parameters in the estimation of the rainfall are the threshold temperatures and proportional constants as shown in **Table 1**. A preliminary study showed, however, that the threshold temperatures to define cold cloud fractional coverage FC do not vary so much within the present data area. Therefore, it is decided that the cloud type discrimination method and the threshold temperatures were to be kept as those in the previous studies as summarized in **Section 2** (Xie[6][7]), and the recalculation of the proportional constants between hourly rainfall and FC are made for the 3 types of rain clouds.

Although the proportional constants can be affected by many meteorological factors such as air temperatures, instability and amount of water vapor, the constants are assumed simply to be dependent upon the latitudes in the present study. Proportional constants between hourly rainfall and FC are thus calculated for various latitudes by using the IR and radar-AMeDAS rainfall data in the meshes with at least 5 gage observations. **Fig. 2a, b** and **c** show the results for the clouds of type A, B and C, respectively. The proportional constants tend to increase linearly from north to south, in general, for all of the three cloud types.

Based upon the results shown in this figure, the proportional constants are then taken as the linear functions of latitude, and the related parameters are determined from the data shown in **Fig. 2** by making linear regression for the three raining types of clouds, whose results are shown in **Table 2**. The slope for the proportional contant of type B (cumulonimbus) is 0.106, which is nearly twice as large as those of type A (cumulus) and C (middle cloud). This means that the development of cumulonimbus is most sensitive to the latitude, which may come from the changes in air temperature and water vapor with latitude.

Therefore, in the present study, rainfall estimation is made from the cold cloud fractional coverage FC for each mesh by applying the proportional constants shown in **Table**

2, which are functions of latitude.

5. Application of the Extended Method

The extended method described in the previous section is then applied to estimate rainfall for the entire area and period and the results are compared with the concurent

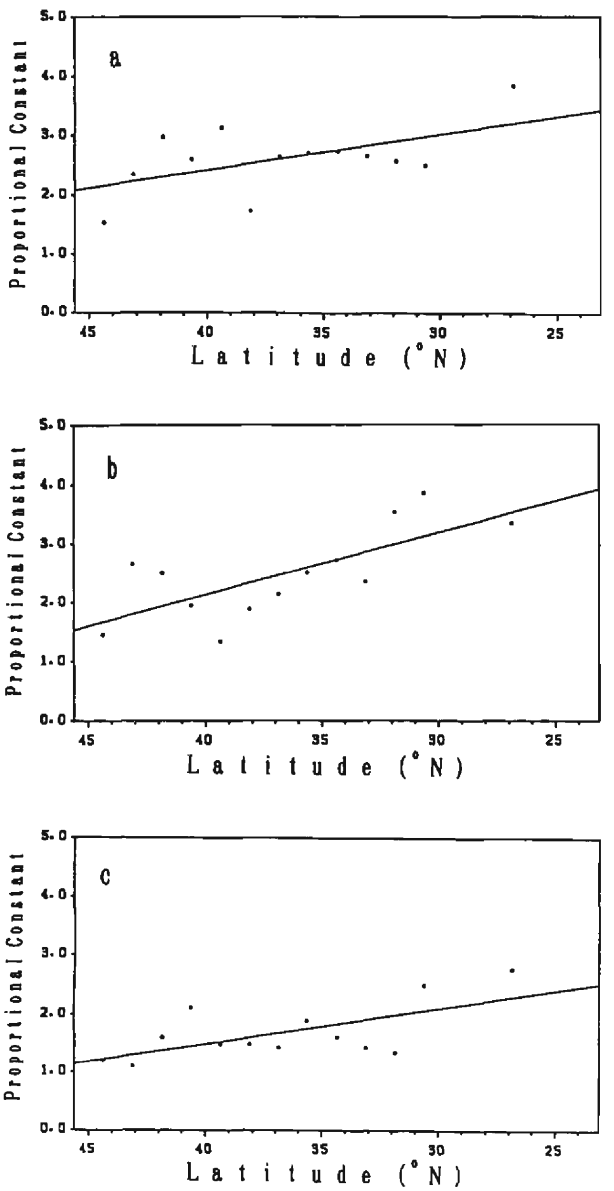

Fig. 2. Proportional constants at various latitudes for the 3 rain types of clouds.

Table 2. Thresholds and Regressional Equations Used in the Extended Method

TYPE	THRESHOLD	REGRESSIONAL EQUATIONS
A	245 K	$E_I=(4.779-0.059\phi)FC_A$
B	235 K	$E_I=(6.383-0.106\phi)FC_B$
C	255 K	$E_I=(3.956-0.062\phi)FC_C$

E_I : IR estimation of hourly rainfall in mm
ϕ : latitude in degree
FC: cold cloud fractional coverage

radar-AMeDAS composite rainfall for meshes over the Japanese islands.

The **Appendix** shows the distributions of estimated daily rainfall for the entire area (middle) and observed daily rainfall over the Japanese islands (left), together with surface weather charts at 0900JST (right) for the period from 1 to 30 June, 1989. The rainfall has been plotted in 8 classes, that is, non-rain; $R<1$ mm; $1\leqq R<2$ mm; $2\leqq R<5$ mm; $5\leqq R<10$ mm; $10\leqq R<20$ mm; $20\leqq R<50$ mm and $R\geqq 50$ mm. The figures plotted above the weather charts are the mean and maximum estimation errors in the meshes over the Japanese islands with at least 5 gages for the day. The Baiu front is located over the main islands of Japan and their adjacent ocean during this period. Lows originating over continental China moved eastward along the front bringing rainfall over the area. A tropical depression also entered this area from the south, landing on Kyushu island, resulting in rainfall in the period from 23 to 25 of June.

Table 3 shows the statistical comparison between our estimation and the radar-AMeDAS rainfall over the Japanese islands for 1, 3, 6, 12, 24 hours and 2, 5, 10, 30 days. The correlation increased from 0.41 for 1 hour to 0.88 for 30 days, while the relative error, defined as the ratio of mean absolute error to the mean of the radar-AMeDAS rainfall, decreased from 107% for 1 hour to 17% for 30 days. The accuracy of our estimation satisfies the useful level of the requirement for climatic study presented

Table 3. Comparison between Radar-AMeDAS composite rainfall and IR Estimation of Rainfall

DURATION	OBS.	EST.	RATIO	CORR.	ERROR	R.E.
1 HR	0.4 mm	0.4 mm	0.98	0.41	0.5 mm	107.2%
3 HR	1.3	1.3	0.98	0.45	1.3	98.1
6 HR	2.6	2.6	0.98	0.48	2.4	91.6
12 HR	5.3	5.2	0.98	0.54	4.3	82.0
24 HR	10.3	10.2	0.99	0.59	7.5	73.1
2 DAY	21.3	20.7	0.97	0.61	13.1	61.6
5 DAY	53.2	51.2	0.96	0.74	18.0	33.8
10 DAY	93.1	91.9	0.99	0.81	25.6	27.5
30 DAY	279.4	275.6	0.99	0.88	48.1	17.2

OBS. : mean of the radar-AMeDAS composite rainfall
EST. : mean of the IR estimation of rainfall
RATIO : ratio of EST. to OBS.
CORR : correlation coefficient between the estimation and the composite rainfall
ERROR: mean of the absolutes of estimation errors compared to the composite rainfall
R.E. : relative error defined as the ratio of ERROR to OBS.

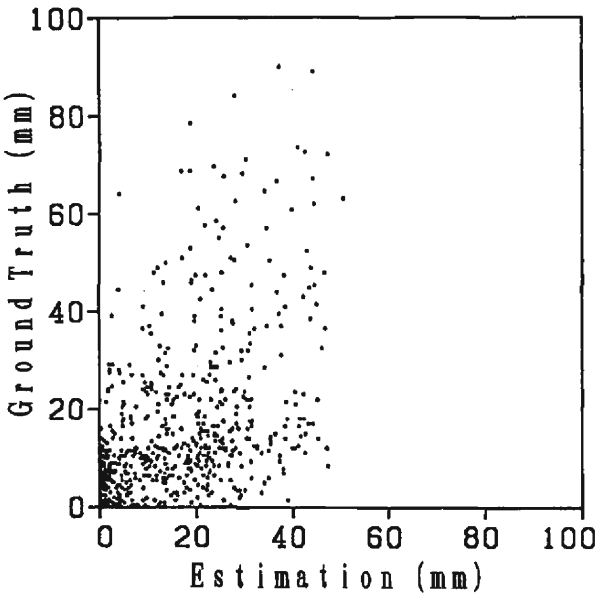

Fig. 3. Scatter of the radar-AMeDAS composite rainfall and IR estimation of rainfall for 24 hours.

by Browning[9], that is 100% and 20% for the 6 hour and the monthly rainfall.

Fig. 3 shows the scatter plot of the estimation and radar-AMeDAS data of daily rainfall. There is a tendency to overestimate in the light rain case and to underestimate in the heavy rain case. There is an obvious upper limit for estimating heavy rainfall, because a linear relation between rainfall and cold cloud fractional coverage (FC) is adpoted and FC is less than unity in the present method.

Fig. 4 shows the same scatter plot for 30 day rainfall. When compared with that for 24 hours as shown in **Fig. 3**, the agreement between estimation and radar-AMeDAS rainfall is improved greatly, especially for the cases of rainfall less than 400 mm/month. However, underestimation still exists for cases of rainfall more than 400 mm/month.

The spatial distribution of the estimation and the radar-AMeDAS rainfall are also compared for 24 hour- and 30 day patterns. As shown in the **Appendix**, the estimated daily rainfall distributions agree relatively well with those of radar-AMeDAS rainfall in general. However, overestimation for light rain and underestimation for heavy rain are found systematically in the edge and central parts of a disturbance, respectively. This is considered to result from the difference in relationship between rainfall and cloud coverage in various parts of a disturbance. The cloud top varies little from the central to the edge parts, while the ascending currents and rainfall concentrate mainly in the central part. As a result, the present method tends to overestimate the rainfall in the edge of disturbances and to underestimate the maximum of the rainfall in the central part.

The estimation error is found to also result from the rain-free assumption in cases with cloud amounts of less than 0.7 (Type S, F) and from error in discrimination of the cloud type. **Table 4** shows rainfall in the cases where the cloud type was determined as

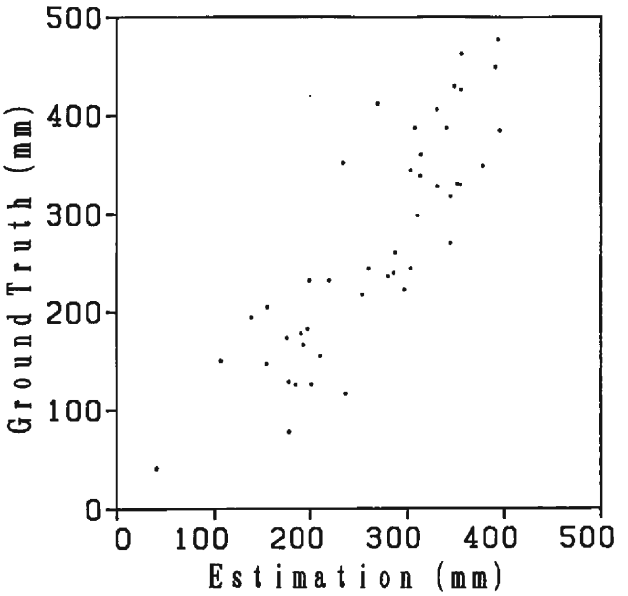

Fig. 4. Same as Fig. 3, for 30 days.

the three types of non-rain clouds from IR data. Among the entire 12268 cases of type S and F, which were estimated as non-rain in the present method, 2864 cases (23%) were rainy with rainfall more than 0.0 mm. Among 2801 cases of type D (Cirrus), which were discriminated also as non-rain, 1532 cases (54.7%) were rainy and 324 cases (11.6%) of rainfall being more than 1.0 mm/hr. These anomalies should be decreased in the future development of the method. In cases with cloud type of A (Cumulus), B (Cumulonimbus) and C (Middle Clouds), the warm cloud case with the fractional coverage (FC) of zero also results in rainfall estimation of 0.0 mm. **Table 5** shows the statistics of real rainfall in such cases which are estimated as non-rain in cloud type A, B

Table 4. The Observed Rainfall for the Case of Non-Rain Cloud Type, S (Clear Sky), F (Fine) and D (Cirrus)

OBSERVED RAINFALL	CLOUD TYPE			
	S	F	D	TOTAL
NON-RAIN	6717	2687	269	10673
R=0 mm	83.2%	64.1%	45.3%	70.8%
LIGHT RAIN	1340	1427	1208	3975
0<R≦1 mm	16.6%	34.0%	43.1%	26.4%
MODERATE RAIN	17	80	297	394
1<R≦5 mm	0.2%	1.9%	10.6%	2.6%
HEAVY RAIN	0	0	27	27
R≧5 mm	0%	0%	1.0%	0.2%
TOTAL	8074	4194	2801	15609

Table 5. Classification of the Rainfall for the Cloud Type of A (Cumulus), B (Cumulonimbus) and C (Middle Clouds) with Estimated Rainfall of 0.0 mm

OBSERVED RAINFALL	CLOUD TYPE			
	A	B	C	TOTAL
NON-RAIN	168	450	549	1167
R=0 mm	56.6%	45.4%	40.4%	44.1%
LIGHT RAIN	118	477	768	1363
0<R≦1 mm	39.7%	48.1%	56.4%	51.4%
MODERATE RAIN	11	65	44	120
0<R≦5 mm	3.7%	6.5%	3.2%	4.5%
HEAVY RAIN	0	0	0	0
R≧5 mm	0%	0%	0%	0%
TOTAL	297	992	1361	2650

and C. About 44% of such cases were truly non-rain, but 56% proved to be rainy. This error in estimation is considered to be caused by error in discrimination of cloud type by the adpotion of determined temperature thresholds.

Geographical distribution of relative error for 24 hour rainfall estimation is shown in **Fig. 5**. The larger error seems to appear in the mountaineous areas. This is considered to result from differences in the relation between rainfall and cloud coverage in mountaineous areas from that in the plain areas.

The agreement in spatial distributions between estimation and radar-AMeDAS

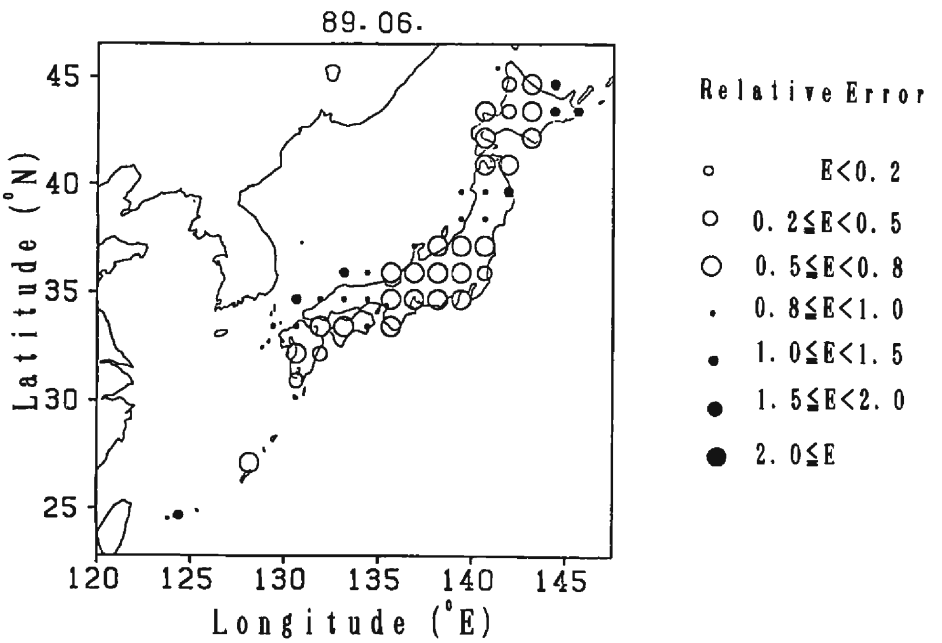

Fig. 5. Distribution of relative error for 24 hour estimation.

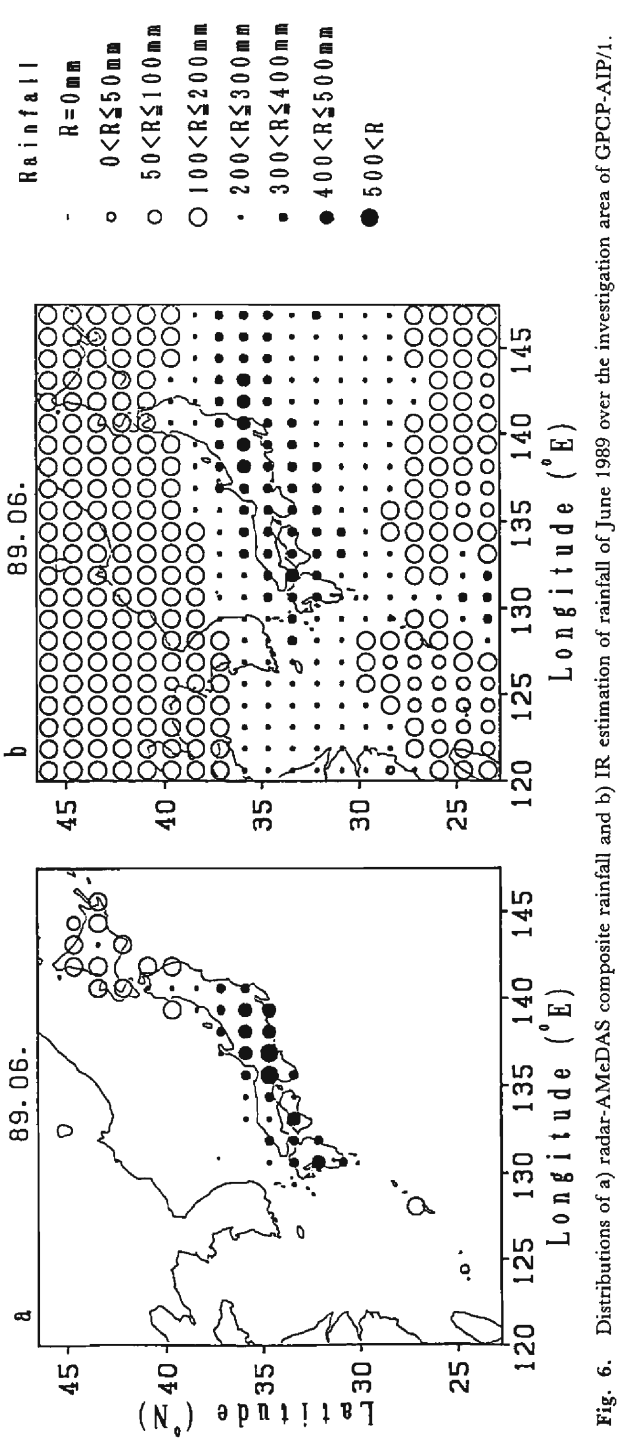

Fig. 6. Distributions of a) radar-AMeDAS composite rainfall and b) IR estimation of rainfall of June 1989 over the investigation area of GPCP-AIP/1.

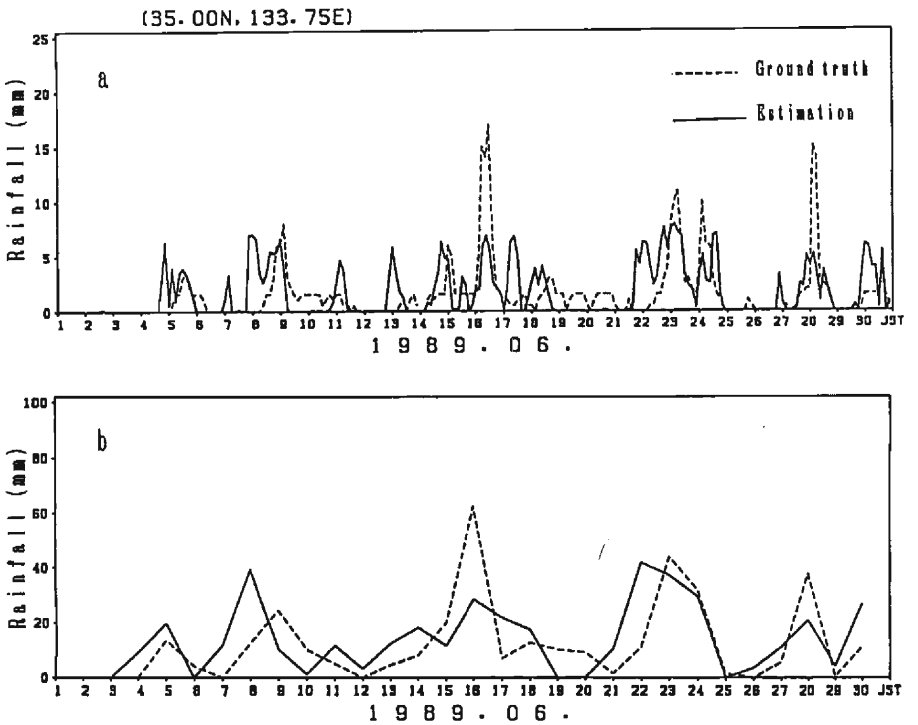

Fig. 7. Time series of radar-AMeDAS composite rainfall (dashed line) and IR estimation of rainfall (thin line) at grid (35.00°–36.25°N; 133.75°–135.00°E) for a) 3 hour and b) 24 hour accumulated data.

rainfall is then investigated for longer periods. **Figs. 6a** and **b** show the total estimation and radar-AMeDAS rainfall distributions for 30 day periods. The rainfall band extending from east to west over Japan and its adjacent ocean has been estimated well, while heavy rainfall more than 500 mm in **Fig. 5a** has been underestimated.

Comparison of time changes of the estimation and radar-AMeDAS rainfall is also made for all meshes over the Japanese islands with at least 5 gages. **Figs. 7a, b** show examples of the time series at mesh (35.00°N–36.25°N; 133.75°E–135.00°E) for 3 and 24 hour rainfall. The rainfall in this mesh during the period from 1 to 30 June, 1989 is characterized by five peaks on 5th, 9th, 16th, 23rd and 28th June, among which four peaks are due to passages of lows along the Baiu front and the other one is due to the landing of a tropical depression.

In the time series of 3 hour rainfall, the estimation reproduces the main peaks of the radar-AMeDAS rainfall; however, the magnitude of the rainfall is greatly underestimated in general. The correlation between the estimation and radar-AMeDAS rainfall is 0.467 and the mean absolute error is 1.7 mm, which is about 105% of the mean of the radar-AMeDAS rainfall in the mesh.

For 24 hr rainfall, the correlation between the estimation and the radar-AMeDAS rainfall is 0.552 and the mean absolute error is 10.5 mm, which is about 81% of the

mean of the rainfall. As shown above, the agreement between the time change pattern has been improved for the 24 hour rainfall. The timing of several peaks, however, is a little different from that of the observation, which is shown to result from the overestimation over edge parts of fronts and lows.

6. Conclusion

The rainfall estimation method developed for the limited areas over Japanese islands (Xie[7]) is extended to estimate the rainfall for wider area surrounding Japan, using the GMS IR imagery data and radar-AMeDAS composite rainfall data in June 1989.

After investigating the relationship between rainfall and clouds over the Japanese islands, threshold temperatures to define cold cloud fractional coverage FC for the three raining types of clouds (A: cumulus; B: cumulonimbus and C: middle cloud) are determined so as to maintain the same as those used in the previous study (Xie[7]). The proportional constants to calculate hourly rainfall from FC are then taken as linear functions of latitude and determined for the three types of clouds.

The extended method provides a relatively good estimation for meshes of 1.25° latitudes × 1.25° longitudes, when compared with the concurrent rainfall obtained from radar-AMeDAS network over Japan. The correlation and relative error are 0.595 and 96% for daily rainfall and 0.88 and 17% for monthly rainfall, which satisfy the useful level of the rainfall data to be used in a climatic study. However, the estimation data tends to underestimate some heavy rainfall peaks and overestimate in light rain cases, especially for shorter estimate periods.

The spatial distribution of estimated rainfall agrees relatively well with that of observed rainfall. The main errors are the underestimation in the center and the overestimation along the edge of a rain area. The time changes of the estimation catch the main peaks in the observation, but the peak values are greatly underestimated in shorter estimate periods.

The estimation errors may also come from the ignorance of the rainfall in the meshes with cloud amounts less than 0.7 and also from the adoption of a simple linear equation to relate hourly rainfall with the cold cloud fractional coverage FC. These points should be improved in further study.

Acknowledgements

The author would like to thank Prof. Y. Mitsuta of the Disaster Prevention Research Institute (DPRI) of Kyoto University for his continous guidance and encouragement during the study. The author is also grateful to Drs. P. A. Arkin and J. E. Janowiak of NMC/NOAA, for supplying the satellite and ground data of AIP/1 and comments on the manuscript of the paper. Discussions with Prof. M. Yamada and other members in the Severe Storm Division of DPRI were very helpful. The computations were performed by FACOM M-730 computer at the Information Processing Center of DPRI.

References

1) Barrett, E. T. and D. W. Martin: The use of satellite data in rainfall monitoring. Academic Press, 1982, pp. 340.
2) Arkin, P. A. and P. E. Ardanuy: Estimating climatic-scale precipitation from space: a review. J. Climate, Vol. 2, 1989, pp. 1229–1238.
3) Griffith, C. G., W. L. Woodley, P. G. Grube, D. W. Martin, J. Stout and D. N. Sikdar: Rain estimation from geosyschronous satellite imagery-visible and infrared studies. Mon. Wea. Rev., Vol. 106, 1978, pp. 1153–1171.
4) Arkin, P. A. and B. N. Meisner: The relationship between large-scale convective rainfall and cloud cover over the western hemisphere during 1982–84. Mon. Wea. Rev., Vol. 115, 1987, pp. 51–74.
5) Xie, P. and Y. Mitsuta: Rainfall estimation from GMS infrared and visible imagery data. Annuals. Disas. Prev. Res. Inst., Kyoto Univ., Vol. 31B-1, 1988, pp. 201–217. (in Japanese)
6) Xie, P.: Nephanalysis of the GMS imagery data. Bull. Disas. Prev. Res. Inst., Kyoto Univ., Vol. 40, 1990, pp. 57–77.
7) Xie, P.: Rainfall estimation in the midlatitudes from GMS infrared imagery data. Bull. Disas. Prev. Res. Inst., Kyoto Univ., Vol. 41, 1991, pp. 109–120.
8) Takemura, Y.: Application of the digital weather dradar. Tenki, Vol.27, pp. 7402–7405. (in Japanese)
9) Browning, K. A.: Rain, rainclouds and climate. Q. J. R. Meteorol. Soc., Vol. 116, 1990, pp. 1025–1051.

Appendix

The distributions of estimated daily rainfall for the entire area (middle), observed daily rainfall over Japanese islands (left) and the surface weather charts at 0900JST (right) for the period from 1 to 30 June, 1989. The rainfall has been plotted into 8 classes: non-rain; $R<1$ mm; $1\text{ mm}\leqq R<2$ mm; $2\text{ mm}\leqq R<5$ mm; $5\text{ mm}\leqq R<10$ mm; $10\text{ mm}\leqq R<20$ mm; $20\text{ mm}\leqq R<50$ mm and $R\geqq 50$ mm. Error (in mm) and relative Error of the estimation of daily rainfall for all meshes over the Japanese islands are plotted over the weather charts.

Appendix

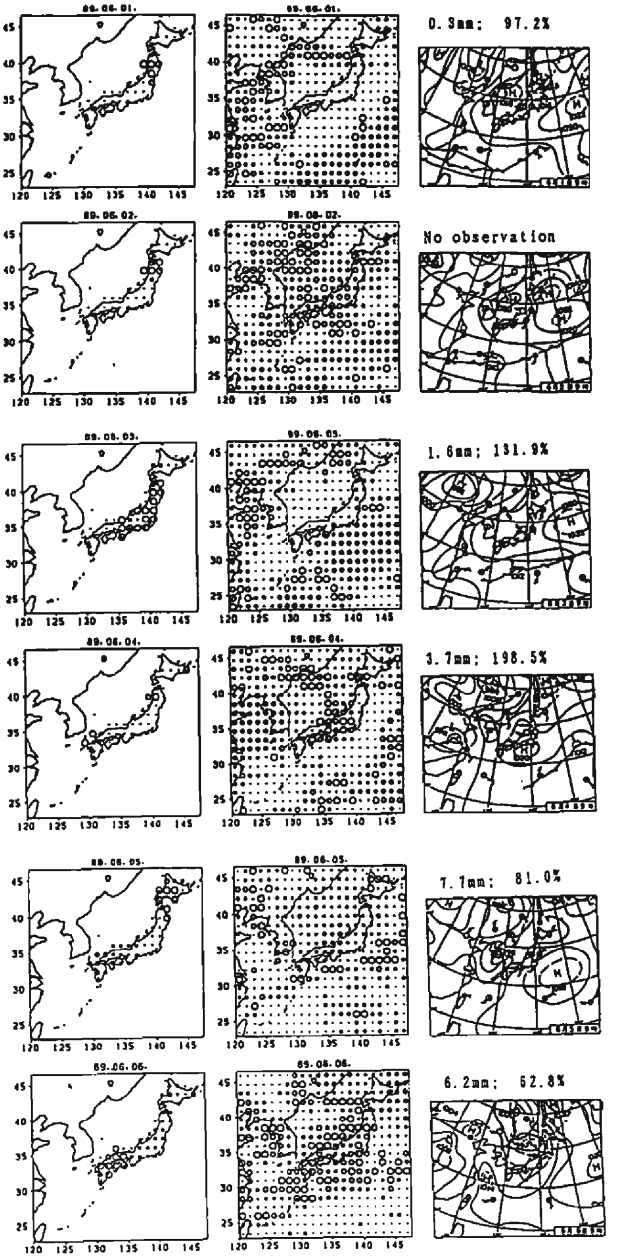
89.06.01.
89.06.01.
0.3mm; 97.2%
89.06.02.
89.06.02.
No observation
89.06.03.
89.06.03.
1.6mm; 131.9%
89.06.04.
89.06.04.
3.7mm; 198.5%
89.06.05.
89.06.05.
7.1mm; 81.0%
89.06.06.
89.06.06.
6.2mm; 62.8%

A–1

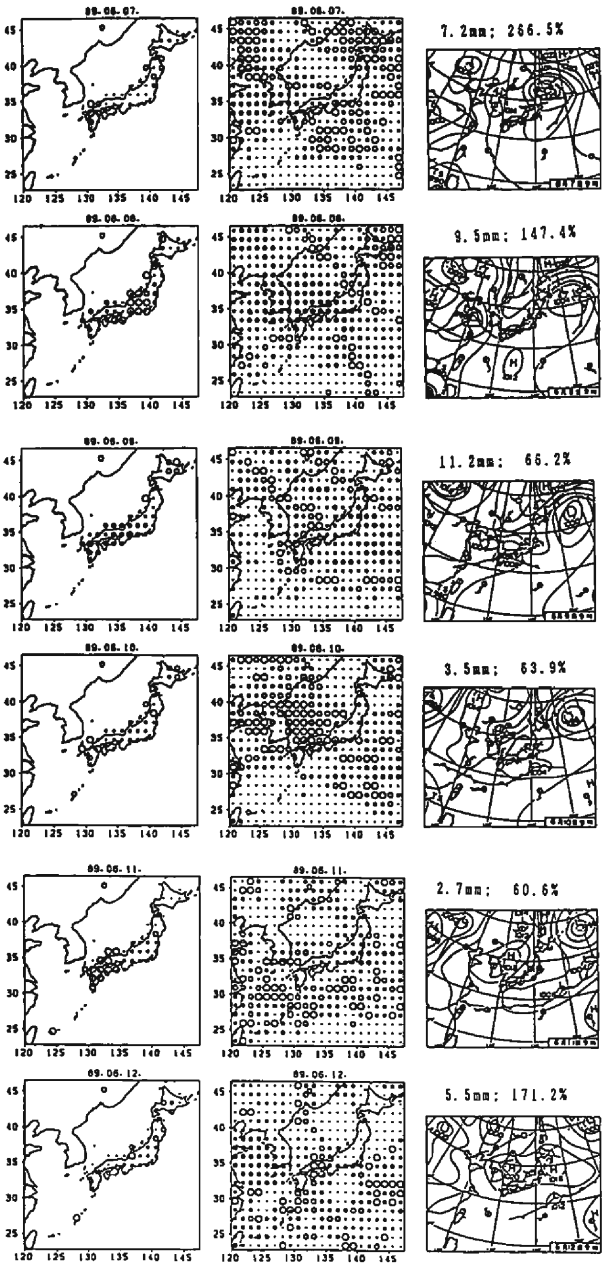
89.06.07.
89.06.07.
7.2mm; 266.5%
89.06.08.
89.06.08.
9.5mm; 147.4%
89.06.09.
89.06.09.
11.2mm; 66.2%
89.06.10.
89.06.10.
3.5mm; 63.9%
89.06.11.
89.06.11.
2.7mm; 60.6%
89.06.12.
89.06.12.
5.5mm; 171.2%

A–2

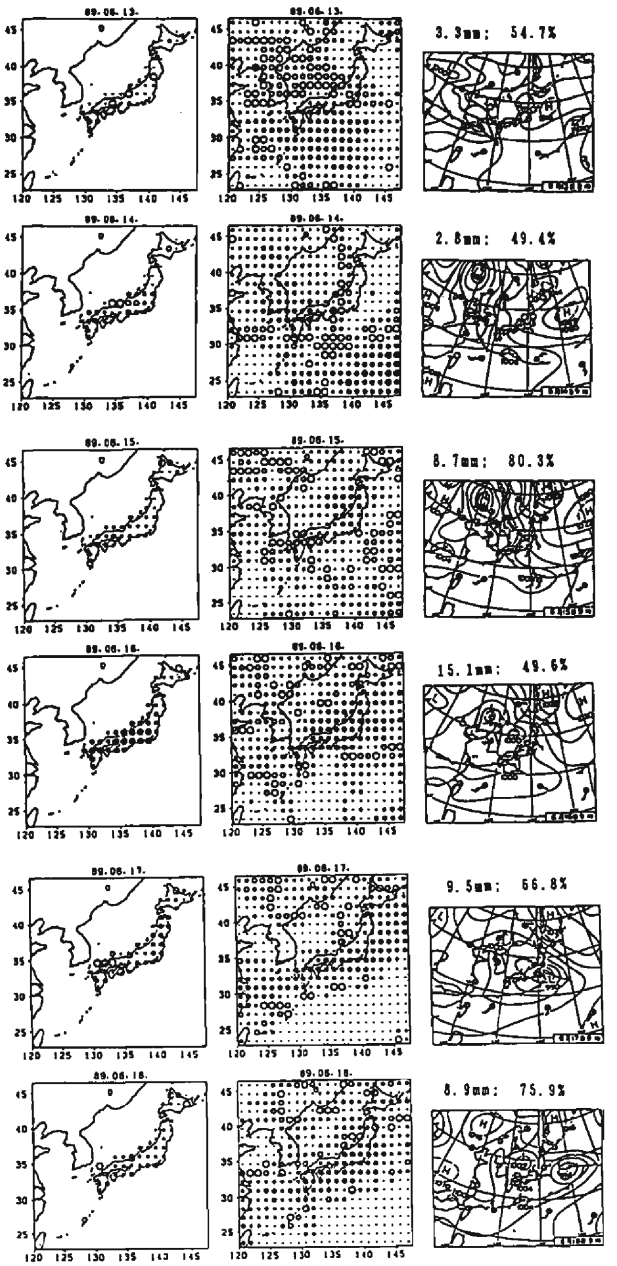
89.06.13.
89.06.13.
3.3mm; 54.7%
89.06.14.
89.06.14.
2.8mm; 49.4%
89.06.15.
89.06.15.
8.7mm; 80.3%
89.06.16.
89.06.16.
15.1mm; 49.6%
89.06.17.
89.06.17.
9.5mm; 66.8%
89.06.18.
89.06.18.
8.9mm; 75.9%

A–3

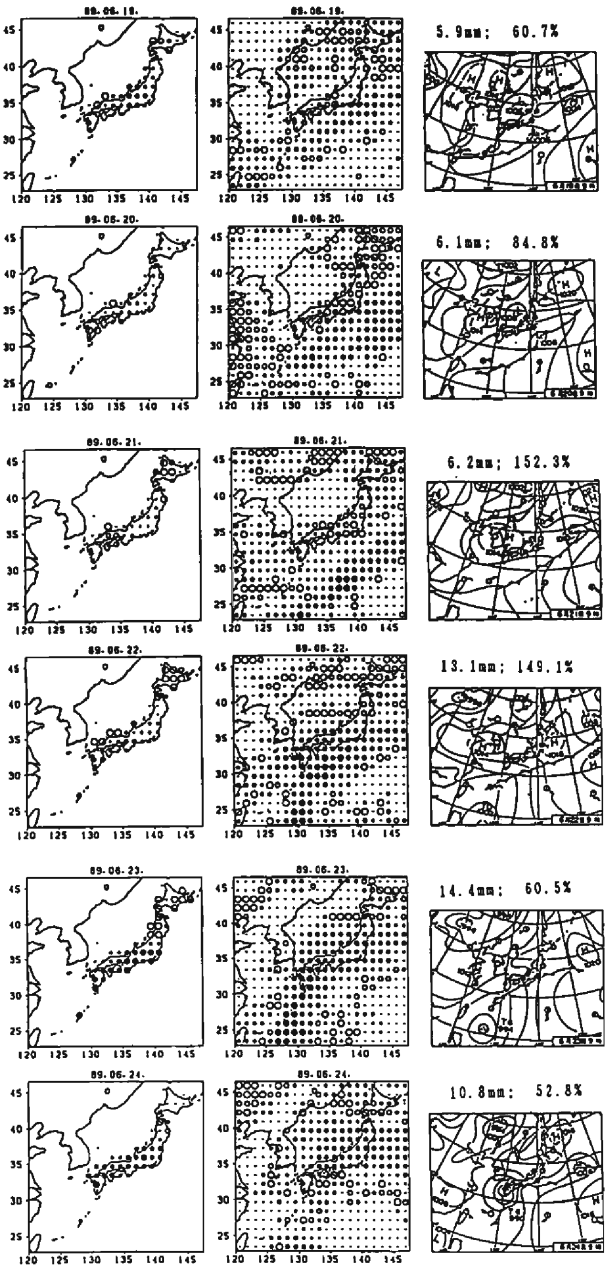
89.06.19.
89.06.19.
5.9mm; 60.7%
89.06.20.
89.06.20.
6.1mm; 84.8%
89.06.21.
89.06.21.
6.2mm; 152.3%
89.06.22.
89.06.22.
13.1mm; 149.1%
89.06.23.
89.06.23.
14.4mm; 60.5%
89.06.24.
89.06.24.
10.8mm; 52.8%

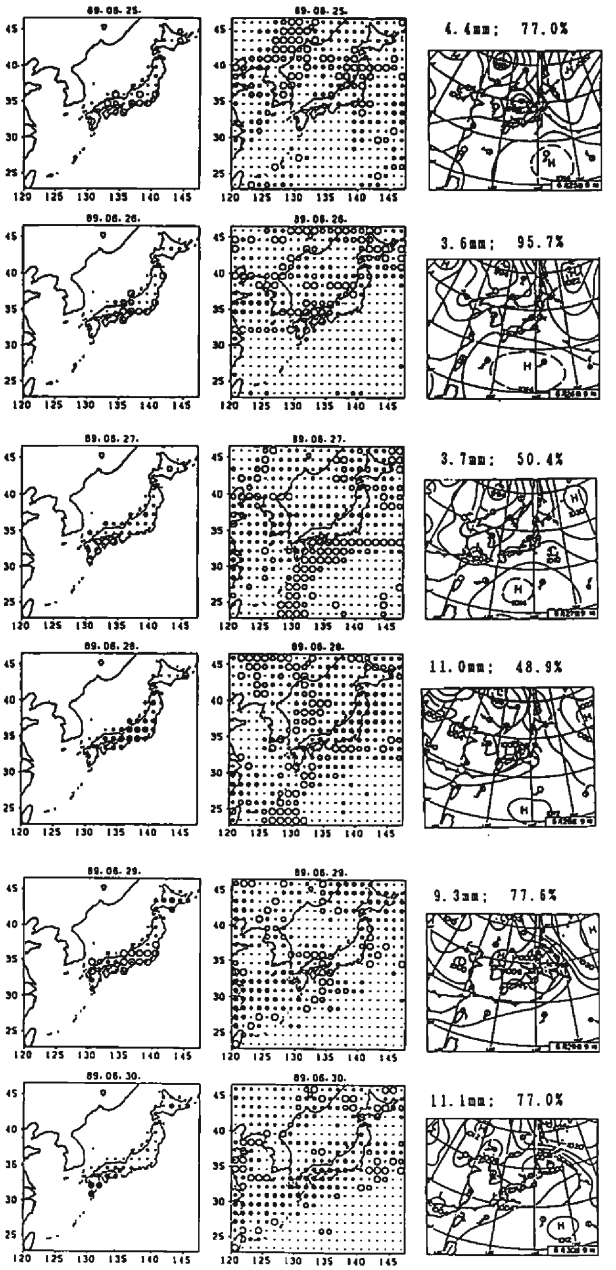
89.06.25.
89.06.25.
4.4mm; 77.0%
89.06.26.
89.06.26.
3.6mm; 95.7%
89.06.27.
89.06.27.
3.7mm; 50.4%
89.06.28.
89.06.28.
11.0mm; 48.9%
89.06.29.
89.06.29.
9.3mm; 77.6%
89.06.30.
89.06.30.
11.1mm; 77.0%

A–5